

## THE ECLIPSING AM HERCULIS VARIABLE H1907+690

R. A. REMILLARD,<sup>1,2</sup> B. A. STROOZAS,<sup>1,3</sup> S. TAPIA,<sup>4</sup> AND A. SILBER<sup>1</sup>*Received 1991 January 10; accepted 1991 April 9*

## ABSTRACT

We report the discovery of an eclipsing cataclysmic variable that exhibits up to 10% circular polarization at optical wavelengths, securing its classification as an AM Herculis type binary. The object, H1907+690, was located with the guidance of X-ray positions from the *HEAO 1* survey. Optical CCD photometry exhibits deep eclipses, from which we derive a precise orbital period of 1.743750 hr. The eclipse duration suggests an inclination angle  $\sim 80^\circ$  for a main-sequence secondary star. The optical flux has been persistently faint ( $V \sim 18$ ) during observations spanning 1987–1990, while the X-ray measurements (one decade earlier) suggest long-term X-ray variability. The polarization and photometric light curves can be interpreted with a geometric model in which most of the accretion is directed toward a single magnetic pole, with an accretion spot displaced  $\sim 17^\circ$  in longitude from the projection of the secondary star on the white dwarf surface. The light curves also indicate that the accreting pole passes behind the white dwarf for 0.32 of the spin period, leading to an estimate of  $18^\circ$  for the colatitude of the accretion spot, relative to the spin axis of the white dwarf. The 3 year stability of the photometric light curve, relative to the eclipse ephemeris, implies spin-orbital synchrony with  $\Delta P/P < 10^{-5}$  ( $3\sigma$ ). Substantial optical flux is observed while the accreting pole is behind the white dwarf, but the origin of this unpolarized continuum remains ambiguous.

*Subject headings:* stars: dwarf novae — stars: eclipsing binaries — stars: individual (H1907+690) — X-rays: binaries

## 1. INTRODUCTION

AM Herculis cataclysmic variables (CVs) are accreting binaries in which a strong magnetic field controls the geometry of the matter flowing from a companion star to a white dwarf (see reviews by Liebert & Stockman 1985; Lamb & Melia 1987). The primary signature of this subclass is circular polarization of the optical continuum (e.g., Tapia 1977; Schmidt, Stockman, & Grandi 1986) caused by cyclotron emission from ionized gas near the polar cap(s) of the white dwarf (surface field  $> 10^7$  G). The radial inflow of matter onto the degenerate dwarf produces high-velocity shock fronts, and magnetic CVs emit substantial X-ray emission as thermal bremsstrahlung radiation with  $kT > 10$  keV (e.g., Ishida et al. 1991). Ten of the 16 known AM Her objects (prior to this report) were identified as a result of their detection as X-ray sources (Ritter 1991). However, the physical models for this class still encounter serious problems regarding the observed ratios of “hard” and “soft” X-ray flux (see Lamb 1985) and the interpretation of the “hard” X-ray luminosity in the context of binary evolutionary models (King & Watson 1987).

Here we report the discovery of the 17th AM Her object, a product of efforts to identify the optical counterparts of “hard” X-ray sources from the *HEAO 1* all-sky survey. Our X-ray identification program is described in detail by Remillard et al. (1986a). X-ray positions are provided by the scanning modulation collimator (MC) experiment on *HEAO 1* (Gursky et al. 1978). The MC instrument produces multiple error

“diamonds” for each X-ray source, and the ambiguity in source location is significantly reduced by the superposition of a coarse error box from another *HEAO 1* experiment, the Large Area Sky Survey (LASS; Wood et al. 1984). Where there are no cataloged objects from known X-ray-emitting classes at the allowed X-ray positions, we search for candidates that show UV excess, emission lines, or evidence of coronal activity. Objects in the first two categories are obtained from Schmidt photography of the field. All candidates are subsequently observed spectroscopically to assess their viability as X-ray counterparts, and this effort includes high-resolution observations of the Ca H and K profiles of bright stars to determine whether there is evidence of an active corona. Previous MC positions led to the discovery of two AM Her objects, EF Eri (2A 0311–227; Griffiths et al. 1979) and BY Cam (H0538+608; Remillard et al. 1986b).

## 2. X-RAY OBSERVATIONS

The MC observations in the vicinity of the LASS source, 1H 1903+689 (Wood et al. 1984), produced an X-ray detection during the first celestial scan of the region by *HEAO 1* on 1978 January 5–31. The MC detection is  $3.5\sigma$  (units are standard deviations in the fluctuations of the X-ray background) for the fine collimator ( $30''$  resolution) and  $2.5\sigma$  for the coarse collimator ( $120''$  resolution), both in the range of 3–13 keV. The second *HEAO 1* scan (6 months later) produced no MC detection, and the combined data significantly diminish the first-scan result. *HEAO 1* did not complete a third scan of this celestial region during its lifetime.

The X-ray positions from the MC, LASS (“1H” from Wood et al. 1984; “2H” from Shrader, Wood, & Matilsky 1986), and also the *Uhuru* survey (“4U”; Forman et al. 1978) are displayed in Figure 1, along with the position of the proposed optical counterpart. The *Uhuru* position misses the CV, but the error box is  $8^\circ$  long, and it intersects the regions near 1H 1840+729 (Wood et al. 1984) to the northwest and 2A

<sup>1</sup> Center for Space Research, Massachusetts Institute of Technology, 77 Massachusetts Avenue, Cambridge, MA 02139.

<sup>2</sup> Guest Observer, Burrell Schmidt telescope, which is jointly operated by Case Western Reserve University and Kitt Peak National Observatory.

<sup>3</sup> Center for EUV Astrophysics, Space Sciences Laboratory, University of California, Berkeley, CA 94720.

<sup>4</sup> Lincoln Laboratory, Massachusetts Institute of Technology, M-232, 244, Wood Street, Lexington, MA 02173.

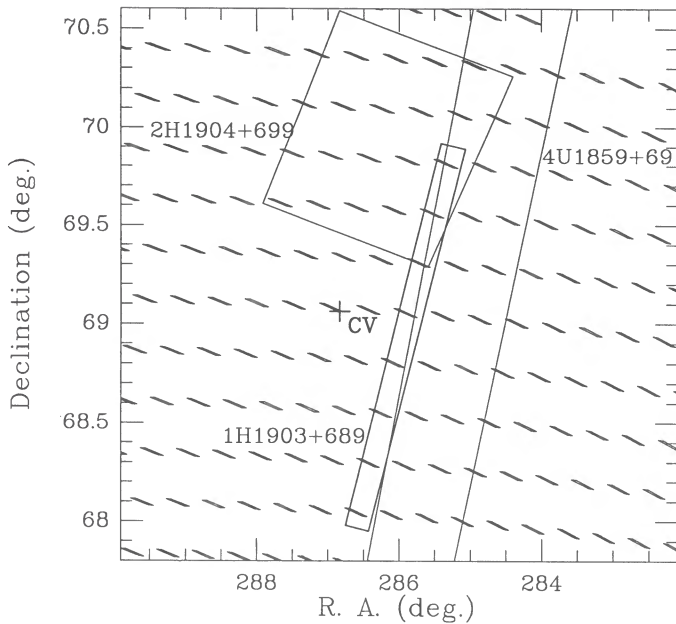


FIG. 1.—X-ray positions in the vicinity of H1907+690 (marked CV). The “1H” and “2H” error boxes denote the *HEAO*-LASS experiment (see text). The *Uhuru* error box (4U) is 8° long and is likely associated with one or two other X-ray sources far north and south of the plotted region. The array of small error “diamonds” is derived from the *HEAO*-MC instrument.

1854+683 (Cooke et al. 1978) to the south. Therefore, the relation between 4U 1859+69 and 1H 1903+689 is very uncertain.

The “1H” and “2H” positions are both derived from the LASS, while the latter positions utilize only the  $1^\circ \times 2^\circ$  modules from that experiment. The LASS observations are contemporaneous with the MC, which produces the field of diamonds shown in Figure 1. The LASS error boxes also miss the CV, but this deviation may well be caused by X-ray variability and/or the fact that the size of the “1H” error box has been underestimated. We have previously proposed X-ray identification with similar offsets, and these judgments have been subsequently confirmed with imaging observations ( $2^\circ \times 2^\circ$  field of view) by *EXOSAT* (e.g., Remillard et al. 1986a; Tuohy et al. 1986). Assuming a Crab-like spectrum, the X-ray flux of 1H 1903+689 in the range of 2–10 keV is  $2.3 \times 10^{-11}$  ergs  $\text{cm}^{-2} \text{s}^{-1}$  (Wood et al. 1984).

### 3. OPTICAL OBSERVATIONS

#### 3.1. Optical Identification

A faint optical candidate with very strong UV flux was located on a photographic plate obtained with the Burrell Schmidt telescope at Kitt Peak National Observatory. The celestial coordinates (epoch 1950) are  $\alpha = 19^{\text{h}}07^{\text{m}}20^{\text{s}}.1$ ,  $\delta = 69^\circ03'50''$ . A finding chart for the CV is provided in Figure 2.

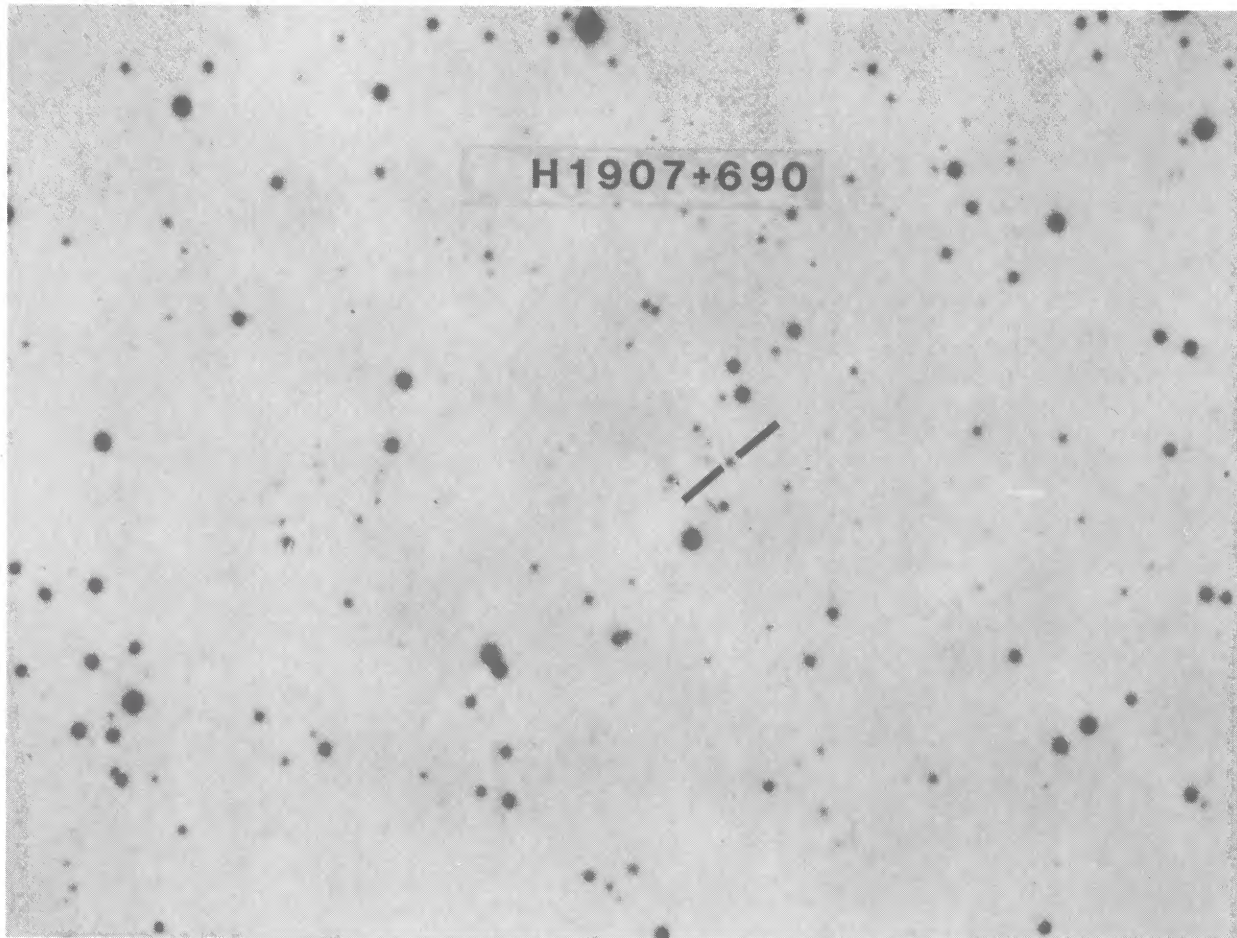


FIG. 2.—Finding chart for H1907+690, photographed from the E print of the Palomar Observatory Sky Survey (© National Geographic Society). North is at the top, and east is to the left. The coordinates (epoch 1950) for the CV are  $\alpha = 19^{\text{h}}07^{\text{m}}20^{\text{s}}.1$ ,  $\delta = 69^\circ03'50''$ .

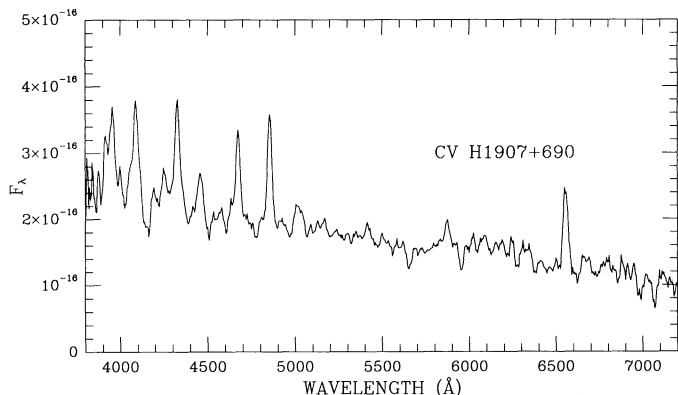


FIG. 3.—Optical spectrum of H1907+690 obtained with the 1.3 m McGraw-Hill Telescope on 1987 July 2. The broadened emission lines of H, He I, and He II are typical of a high-excitation cataclysmic variable.

We designate this object H1907+690 to reflect the true position of the *HEAO 1* source rather than the center of the X-ray error box, (1H 1903+689). Spectroscopy was undertaken on 1987 July 2 using the Mark II Reticon scanner (Shetman & Hiltner 1976) and the 1.3 m McGraw-Hill Telescope at the MDM<sup>5</sup> Observatory. The average spectrum for 200 minutes of integration is shown in Figure 3. The spectrum is typical of a high-excitation CV with strong emission lines of H, He I, and He II.

The photon-counting capability of the Mark II spectrograph, along with photometric observing conditions, provided a record of the optical light curve while the spectrum was being accumulated. Despite the low count rate from spectroscopy of an 18th magnitude object with a 1.3 m telescope, we recognized deep eclipses with a period near 105 minutes. In addition, the CV appeared to be noticeably redder when brighter, suggesting the strong possibility of an AM Her binary, where the light curve is driven by the orientation of the accretion column and

the optically bright phases are dominated by cyclotron harmonics that are often enhanced in the red part of the spectrum (e.g., Wickramasinghe, Tuohy, & Visvanathan 1987).

It will be shown in § 3.3 that H1907+690 is a confirmed AM Her object. The discovery of a magnetic CV within an MC error diamond is strong motivation to believe that the X-ray source has been identified, but some caution must be given, since the object has appeared relatively faint during our observations, and there is some possibility that a distant CV may lie, by chance, within one of the MC error diamonds. If we hypothesize that the 18th magnitude is a “normal” AM Her object at a distance  $\sim 600$  pc, then the estimated surface density of all AM Her objects within this distance is  $\sim 2 \times 10^{-3}$  per square degree (Patterson 1984). At this surface density, we determine a total expectation value of 0.02 for finding similar or brighter AM Her CVs by chance during our entire *HEAO 1* identification program (200 sources, each surrounded by 40 MC error diamonds, accumulating a total surface area  $\sim 9$  square degrees). Therefore, we conclude that the CV is the optical counterpart of the *HEAO 1* X-ray source. Further discussions concerning the ratio of the X-ray to the optical flux are given in § 4.

### 3.2. CCD Photometry

The recognition of eclipses prompted further efforts to obtain light curves with imaging CCD cameras. The observations were spaced by a wide variety of time scales, to ensure a precise and unique determination of the orbital period of the binary system. A journal of observations and eclipse times is provided in Table 1. The data were obtained with either the 1.3 m or the 2.4 m telescopes at MDM Observatory, using the TI 4849 or the Thomson CCD detectors. The relative light curves are computed with an algorithm that scales the intensity and location of a given star to secure a minimum  $\chi^2$  fit to the point-spread profile of a designated template star. For each CCD image, the profile is specified with a two-dimensional Gaussian and interpolations for an empirical table of residuals, as implemented in the program DAOPHOT (Stetson 1987). The template star is the bright object 0.9 south-southeast of the CV in Figure 2. The uncertainty for individual points in the CV

<sup>5</sup> The Michigan-Dartmouth-MIT (MDM) Observatory is operated by a consortium consisting of the University of Michigan, Dartmouth College, and the Massachusetts Institute of Technology.

TABLE 1  
H1907+690 ECLIPSES

Observation Date	Telescope (m)	Instrument	Numbers of Eclipses	Epoch <sup>a</sup> (HJD)	Residuals <sup>b</sup>
1987 Jun 28 .....	1.3	Mark II spectrograph	1	6974.9293	0.002
1987 Jun 29 .....	1.3	Mark II spectrograph	1	6975.9461	-0.003
1987 Jul 2 .....	1.3	Mark II spectrograph	3	6978.8524	-0.003
1987 Jul 5 .....	1.3	Mark II spectrograph	1	6981.9038	-0.005
1988 May 26 .....	1.3	TI CCD	2	7307.8402	0.001
1988 May 29 .....	1.3	TI CCD	2	7310.8190	0.000
1988 Aug 18 .....	2.4	TI CCD	1	7391.9759	-0.002
1988 Nov 28 .....	1.3	RCA CCD	1	7493.6220	-0.001
1988 Nov 30 .....	1.3	RCA CCD	1	7495.5840	0.002
1989 Jun 4 .....	2.4	ACIS CCD	2	7681.7294	0.003
1989 Jun 5 .....	2.4	ACIS CCD	3	7682.7465	0.002
1990 May 23 .....	2.4	TI CCD	1	8034.9112	0.000
1990 Jun 20 .....	1.3	MINIPOL	2	8062.8115	0.004
1990 Jun 22 .....	1.3	MINIPOL	2	8064.7730	0.002
1990 Jul 2 .....	1.3	TI CCD	1	8074.9454	0.009

<sup>a</sup> Heliocentric Julian Day of eclipse midpoint after 2,440,000, with an uncertainty of about 0.0002 days.

<sup>b</sup> Residuals are the difference between ephemeris prediction and the eclipse epoch given in the preceding column, units of orbital phase. The predicted eclipse times are derived from the best-fit values, viz.,  $P = 0.07265625$  days and epoch HJD 2,447,681.729164.

light curve are the rms fluctuations of field stars with brightness similar to the CV in any given filter, on any given night.

A 5 hr sample of the light curve of H1907+690 is displayed in Figure 4. The data, which were obtained in the *I* band, clearly show three sequential eclipses at a period  $\sim 1.74$  hr. The individual observing runs produce very similar results, and we are able to determine a very precise period for the binary system as follows. All of the data, which include 24 eclipses, were corrected to the heliocentric reference frame; then the observations of different epochs and with different filters were normalized to a value of 1.0 at phase 0.5 (mideclipse defines phase 0.0). We then derived the orbital period by computing the  $\Theta$ -static of Stellingwerf (1978) for trial periods near 1.74 hr. This method folds the light curve into "phase bins" and computes the bin-averaged variance ( $\Theta$ ), normalized by the variance of the entire data set, for each trial period. The results are displayed in Figure 5; the bin-averaged variance is minimized at a period of 1.743750 ( $\pm 0.000004$ ) hr, with a central epoch (HJD) 2,447,681.72916 ( $\pm 0.00010$ ). The period uncertainty is estimated from the profile of the  $\Theta$ -static near the minimum value. The orbital period is corroborated by the residuals between the observed and predicted eclipses given for each observing run in Table 1.

The color dependence of the light curve is evident in Figure 6. The observations of 1988 May included the use of both *V* and *I* filters, and the results are representative of the behavior of H1907+690 during other epochs as well. The maxima are more pronounced in the *I* band, especially the pre-eclipse maximum, confirming the earlier suggestions of a correlation between optical brightness and a red color index within each orbital cycle. The brightness level at phase 0.5 has been in the range of  $17.6 < V < 18.4$ .

### 3.3. Optical Polarimetry

Finally, circular polarimetry of H1907+690 was performed during 1990 June with the MINIPOL polarimeter (Frecker & Serkowski 1976) on the 1.3 m McGraw-Hill Telescope at MDM Observatory. The observations were conducted on 1990 June 19, 20, and 22 (UT), using a 15" aperture and a broad filter with transmission in the wavelength range 5000–9000 Å. A total of 7.8 hr of observations were obtained during clear and moonless conditions. On each night we also measured the circular polarization of GRW +70°8247, which

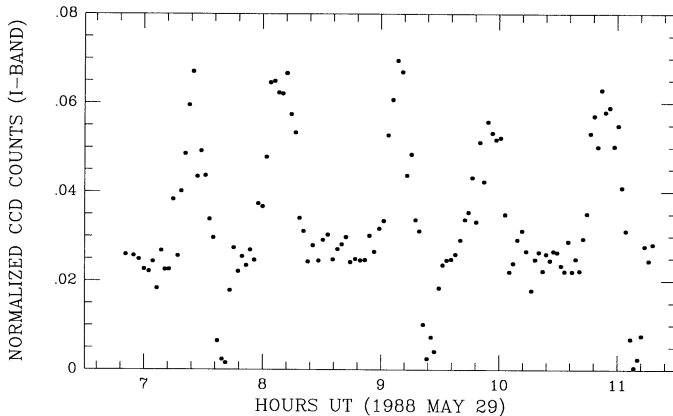


FIG. 4.—Optical light curve of H1907+690. Three consecutive eclipses are evident with a period  $\sim 1.74$  hr.

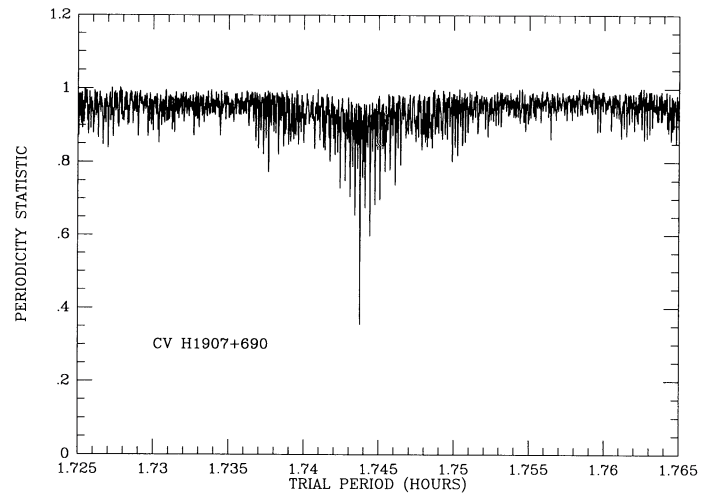


FIG. 5.—A unique period is derived from photometric data that spans 3 years and includes 24 eclipses (see Table 1). Heliocentric corrections were applied before computing the  $\Theta$ -static of Stellingwerf (1978) to search for the period value that minimizes the variance locally averaged over 50 phase bins. The best period is 1.743750 ( $\pm 0.000004$ ) hr.

yielded an average value of  $-2.66\%$  ( $\pm 0.09\%$ ) in the same bandpass.

The circular polarization of H1907+690, folded at the photometric period, is shown in Figure 7. The polarization reaches 10% near binary phase 0 and is visible during  $\sim 0.68$  of each orbit. There is far less circular polarization on the opposite hemisphere of the white dwarf, with a net value of  $-1.3\% \pm 0.6\%$  for the range 0.4–0.6 in binary phase.

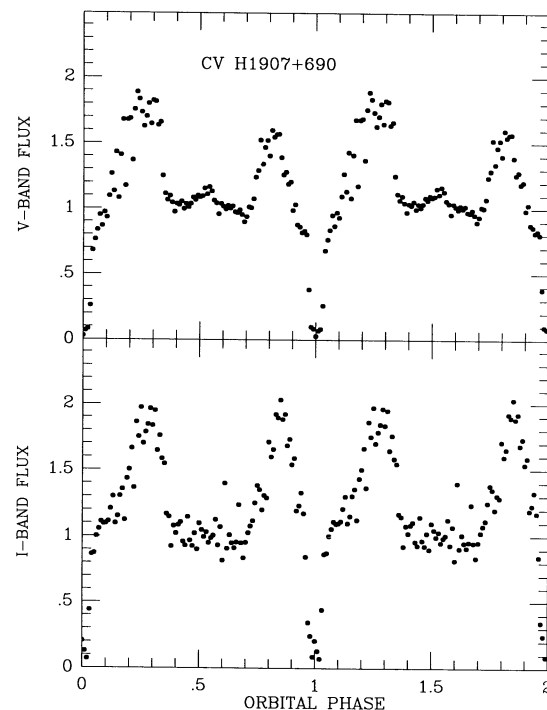


FIG. 6.—Folded light curves in *V* and *I* bandpasses for CCD observations obtained during 1988 May. Phase 0.0 corresponds to the time of mideclipse. The bright portions of the light curve are interpreted as cyclotron beaming with harmonics that dominate in the red part of the spectrum.

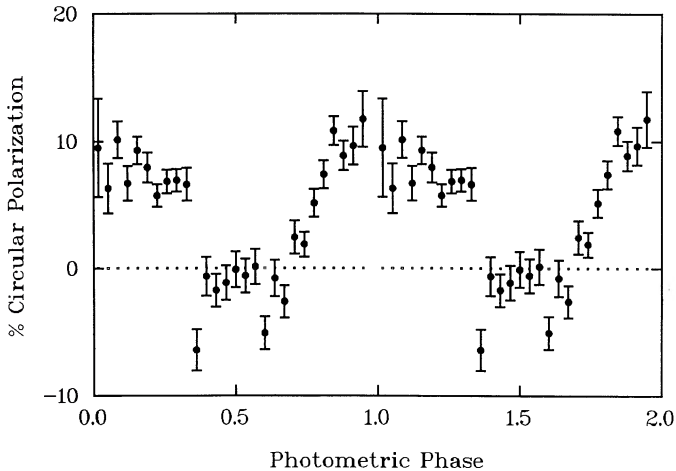


FIG. 7.—Circular polarization obtained in 1990 June, confirming that H1907+690 is an AM Her binary. The measurements were unfiltered, the data were folded at the photometric period, and phase 0.0 corresponds to the time of mideclipse.

#### 4. DISCUSSION

The comparison of the maximum X-ray flux (2–10 keV) with our optical measurements (4000–7000 Å) reveals a flux ratio,  $f_x/f_{opt} \sim 40$ , which is a factor of 10 larger than expected (e.g., Remillard et al. 1989b). Either the first *HEAO 1* scan captured the source in a state of enhanced luminosity (X-ray and optical) or the X-ray efficiency of this AM Her binary is unusually high. This situation is not unprecedented, as similar implications were encountered with a previous AM Her discovery, 1E 1048+542 (Morris et al. 1987), located with the imaging capability of the *Einstein Observatory*.

The discovery of H1907+690 marks the fourth example of an eclipsing AM Her binary (see Biermann et al. 1985; Bailey et al. 1988; Ferrario et al. 1989). The eclipse appears to be nearly total, with  $V > 20.8$  at minimum light. The phase duration is 0.066, as measured from the FWHM of the steepest portions of the light curve (Fig. 6). The orbital period provides an estimate of the radius of the secondary star relative to the binary separation (Patterson 1984). For an unevolved secondary star, the mass ratio (secondary/white dwarf) is expected to be roughly in the range 0.2–0.3, and the observed eclipse duration then implies an inclination angle  $\sim 80^\circ$ .

The spectra obtained during eclipses show no evidence of absorption features from the companion star, but the wavelength coverage has been limited to regions blueward of 7000 Å, while the continuum flux from the anticipated  $\sim$ dM6 companion is largely redward of this limit (see Puchnarewicz et al. 1990). The deep eclipses in the *I* band together with the orbital period provide a rough estimate of the lower limit for the distance to the binary system, if the secondary star is again presumed to lie on the main sequence. The orbital period suggests a secondary star with  $M_V < 16$  (Patterson 1984), which implies  $M_I < 12$  (Young & Schneider 1981). At mideclipse the upper limit ( $3\sigma$ ) for the brightness of the secondary star is  $I \geq 19.5$ , which then implies that the distance to the binary system is at least 300 pc.

The temporal behavior of H1907+690 displayed in Figures 6 and 7 suggests that the accretion is dominated by a single magnetic pole. Positive circular polarization reaches a maximum while we view the white dwarf's hemisphere that faces the secondary star, while there is very little polarization

detected on the opposite hemisphere. The offset between mideclipse and the midpoint of circular polarization (Fig. 7) is only  $\sim 17^\circ$  in longitude. The symmetry of the photometric peaks (Fig. 6) is similarly offset from mideclipse, and the pair of bright spots may be naturally explained by “cyclotron beaming,” i.e., the intensity maxima coincide with a transverse view of the magnetic field at the accretion spot when the latter is near the limb of the white dwarf.

Despite the lack of linear polarization measurements of H1907+690 (see Stockman 1977), we may take advantage of the simplicity of single-pole accretion in an eclipsing binary system and derive the colatitude ( $\delta$ ) of the accretion spot (i.e., the angle between the accretion spot and the spin axis of the white dwarf). The duration of unpolarized emission and the time between the maxima in the optical photometry (through phase 0.5) both describe a phase interval,  $\Delta\phi \sim 0.32$ ; the accreting pole is apparently behind the white dwarf during this time. If we assume that the binary and white dwarf spin axes are coaligned and that the cyclotron-emitting region is very close to the white dwarf surface, then

$$\tan \delta = -1.0 / \{(\tan i) \cos [180^\circ(1 - \Delta\phi)]\},$$

where  $i$  is the binary inclination angle, estimated above at  $80^\circ$ . The colatitude of the accretion spot is then  $\delta \sim 18^\circ$ .

Since the photometric maxima in the light curve are attributed to cyclotron beaming, their modulation is driven by the rotation of the white dwarf rather than the orbital motion of the binary system. The long-term stability of the detailed shape of the optical light curve is therefore evidence of spin-orbital synchrony. We have further calculated the  $\Theta$ -statistic (see § 3.2) for the photometric light curve after removing all of the data with phases  $\pm 0.05$  relative to the eclipses by the secondary star. The derived spin period is  $1.743745 \pm 0.000005$  hr. Within this interpretation, the fractional difference between the spin and orbital periods is less than  $1.3 \times 10^{-5}$  at the  $3\sigma$  level of confidence.

If the optical continuum were strongly dominated by cyclotron emission, one would expect the optical flux of H1907+690 to be very weak when the accretion spot is hidden from our view (phase interval 0.34–0.66). In Figure 6 it is clear that there is substantial remaining light, although the continuum is more blue ( $B-V \sim 0.2$ ;  $V-R \sim 0.0$ ) compared with the spectra of the bright spots ( $B-V \sim 0.45$ ;  $V-R \sim 0.25$ ). The estimated lower limit for the distance to the binary system (300 pc) implies that the absolute brightness at phase 0.5 is  $M_V < 10.2$ . This luminosity limit is derived from the MINIPOL data that also exclude significant circular polarization at phase 0.5, eliminating the possibility of substantial emission from the second magnetic pole. It is unlikely that the nonaccreting hemisphere of the white dwarf would be so luminous (Liebert 1980), and the spectra accumulated during this time continue to resemble Figure 3. The origin of this continuum may then be either thermal emission from the extended accretion column above the white dwarf surface, or reprocessed emission from the heated face of the secondary star (Liebert & Stockman 1985). The current data are insufficient to exclude either of these alternatives. The simplicity of the accretion geometry and the fortune of viewing both binary and accretion-spot eclipses in the case of H1907+690 (and also EXO 02343–5232; Bailey et al. 1988) may provide a means of investigating the origin or the unpolarized optical continuum in AM Her stars.

Wendy Roberts measured the optical position and prepared the finding chart. We thank Bob Barr and Larry Breuer of MDM Observatory for their invaluable assistance. This work

was supported in part by NASA grant NAG8-493 and NSF grant AST 86-12572, and by the Department of the Air Force.

## REFERENCES

- Bailey, J., Wickramasinghe, D. T., Hough, J. H., & Cropper, M. 1988, *MNRAS*, 234, 19P
- Biermann, P., et al. 1985, *ApJ*, 293, 303
- Cooke, B. A., et al. 1978, *MNRAS*, 182, 489
- Ferrario, L., Wickramasinghe, D. T., Bailey, J., Tuohy, I. R., & Hough, J. H. 1989, *ApJ*, 337, 832
- Forman, W., Jones, C., Cominsky, L., Julien, P., Murray, S., Peters, G., Tananbaum, H., & Giacconi, R. 1978, *ApJS*, 38, 357
- Frecker, J. E., & Serkowski, K. 1976, *Appl. Optics*, 15, 605
- Griffiths, R. E., Ward, M. J., Blades, J. C., Wilson, A. S., Chaisson, L., & Johnston, M. D. 1979, *ApJ*, 232, L27
- Gursky, H., et al. 1978, *ApJ*, 223, 973
- Ishida, M., Silber, A., Bradt, H. V., Remillard, R. A., Makishima, K., & Ohashi, T. 1991, *ApJ*, 367, 270
- King, A. R., & Watson, M. G. 1987, *MNRAS*, 227, 205
- Lamb, D. Q. 1985, in *Cataclysmic Variables and Low Mass X-Ray Binaries*, ed. D. Q. Lamb & J. Patterson (Dordrecht: Reidel), 179
- Lamb, D. Q., & Melia, F. 1987, *Space Sci. Rev.*, 131, 511
- Liebert, J. 1980, *ARA&A*, 18, 363
- Liebert, J., & Stockman, H. S. 1985, in *Cataclysmic Variables and Low Mass X-Ray Binaries*, ed. D. Q. Lamb & J. Patterson (Dordrecht: Reidel), 151
- Morris, S. L., Schmidt, G. D., Liebert, J., Stocke, J., Gioia, I. M., & Maccacaro, T. 1987, *ApJ*, 314, 641
- Patterson, J. 1984, *ApJS*, 54, 443
- Puchnarewicz, E. M., Mason, K. O., Murdin, P. G., & Wickramasinghe, D. T. 1990, *MNRAS*, 244, 20P
- Remillard, R. A., Bradt, H. V., Buckley, D. A. H., Roberts, W., Schwartz, D. A., Tuohy, I. R., & Wood, K. 1986a, *ApJ*, 301, 742
- Remillard, R. A., Bradt, H. V., McClintock, J. E., Patterson, J., Roberts, W., Schwartz, D. A., & Tapia, S. 1986b, *ApJ*, 302, L11
- Ritter, H. 1991, *A&AS*, 85, 1179
- Schmidt, G. D., Stockman, H. S., & Grandi, S. A. 1986, *ApJ*, 300, 804
- Shectman, S. A., & Hiltner, W. A. 1976, *PASP*, 88, 960
- Shrader, C. R., Wood, K. S., & Matilsky, T. 1986, *ApJS*, 61, 353
- Stellingwerf, R. F. 1978, *ApJ*, 224, 953
- Stetson, P. B. 1987, *PASP*, 99, 191
- Stockman, H. S. 1977, *ApJ*, 218, L57
- Tapia, S. 1977, *ApJ*, 212, L125
- Tuohy, I. R., Buckley, D. A. H., Remillard, R. A., Bradt, H. V., & Schwartz, D. A. 1986, *ApJ*, 311, 275
- Wickramasinghe, D. T., Tuohy, I. R., & Visvanathan, N. 1987, *ApJ*, 318, 326
- Wood, K., et al. 1984, *ApJS*, 56, 507
- Young, P., Schneider, D. P. 1981, *ApJ*, 247, 960